Eleventh International Conference on CFD in the Minerals and Process Industries
CSIRO, Melbourne, Australia
7-9 December 2015

SIMULATION AND VALIDATION OF TURBULENT GAS FLOW IN A CYCLONE USING CAELUS

Darrin W. STEPHENS [1*], Chris SIDEROFF[2] and Aleksandar JEMCOV[3]

[1] Applied CCM Pty Ltd, Dandenong North, Victoria, 3175, AUSTRALIA

[2] Applied CCM, Ottawa, ON K1J 6K3, CANADA

[3] Aerospace and Mechanical Engineering, University of Notre Dame, Notre Dame, IN 46556, USA
*Corresponding author, E-mail address: d.stephens@appliedccm.com.au

ABSTRACT

Cyclones play a dominant role in the industrial separation of dilute particles from an incoming gas flow. The complex swirling flow in cyclones provides significant challenges for turbulence modelling in CFD. This paper presents a single phase transient solver developed using the Caelus library. The solver predictions using *k*-ω SST with and without curvature corrections, Reynolds Stress Model (LRR) and Large Eddy Simulation (Smagorinsky and coherent structure) turbulence models are compared against laser velocity measurements to investigate the level of accuracy afforded by each turbulence model. The *k*-ω SST model without any curvature corrections produced the poorest predictions of the flow field, whilst the coherent structure LES was found to be in excellent agreement with the experimental measurements.

NOMENCLATURE

a_1	SST *k*-ω turbulence model constant
a_{ij}	anisotropy tensor
c_{r1-3}	curvature correction constant
C_{RC}	Hellsten curvature correction constant
C_{scale}	curvature correction constant
C_s	SGS model constant
C_{SM}	Coherent structure model constant
C_{1-5}	SSG/LRR Reynolds stress model constants
C_1^*	SSG/LRR Reynolds stress model constant
C_3^*	SSG/LRR Reynolds stress model constant
C_2^{LRR}	SSG/LRR Reynolds stress model constant
d	wall distance
D_{ij}	diffusion tensor
D	diffusion model constant
$\mathbf{D}$	rate of deformation tensor
E	magnitude of shear rate
f	body force
f_r	streamline curvature strength
$f_{rotation}$	streamline curvature strength
F_1	First SST blending function
F_2	Second SST blending function
F_4	Hellsten curvature correction function
F_{CS}	Coherent structure function
k	turbulence kinetic energy
p'	modified pressure
P_{ij}	production tensor
P_k	shear production of turbulence
Q	second invariant
r^*	curvature correction function
$\tilde{r}$	curvature correction function
R_i	Richardson number
R_{ij}	Reynolds stresses
S_{ij}	strain rate tensor
t	time
u	velocity
α_ω	SST *k*-ω turbulence model constant
β^*	SST *k*-ω turbulence model constant
β_ω	SST *k*-ω turbulence model constant
δ_{ij}	Kronecker delta
Δ	top-hat filter width
ε_{ij}	dissipation tensor
ε	isotropic turbulence dissipation rate
ν	kinematic viscosity
ν_t	kinematic turbulent viscosity
ξ	pressure loss coefficient
Π	pressure-strain correlation
σ_d	SSG/LRR-ω turbulence model constant
σ_k	*k*-ε turbulence model constant
σ_ω	SST *k*-ω turbulence model constant
τ_{ij}	stress tensor
ϕ	blended model constant
ϕ_1	inner model constant
ϕ_2	outer model constant
ω	turbulence frequency
Ω_{ij}	vorticity tensor

Subscripts

i, *j*, *k*	components
mag	magnitude
SGS	Subgrid scale

Superscript

$(\bar{})$	Favre-averaged
rot	rotation

INTRODUCTION

Cyclones play a dominant role in the industrial separation of dilute particles from an incoming gas flow. The incoming flow enters tangentially and accelerates on its way down into a conical section. This acceleration results in a strong swirling flow. The particle laden flow escapes through the bottom outlet while the rest of the flow reverses and swirls about the centreline towards the upper exit through the vortex finder. Due to the inherent presence of high swirl and very large curvature of streamlines within the flow, modelling such flow presents a challenge to this date. Boysan et al. (1984) conducted one of the first CFD simulations and found the standard *k-ε* turbulence model is inadequate to simulate such flows. The high swirl leads to excessive turbulent viscosities and incorrect tangential velocity patterns in CFD simulations. Witt et al. (1999) showed the accuracy of the numerical solution can be improved by using a Reynolds Stress Model for the turbulence. Stephens and Mohanarangam (2010) showed for a hydrocyclone it was possible to get accurate mean flow behaviour using a two-equation SST turbulence model corrected for streamline curvature.

The main objective of this paper is to investigate the effect turbulence model selection has on the predicted mean flow behaviour within a gas cyclone. In order to verify the validity of the numerical simulations, the results were compared against the experimental data of Witt et al. (1999).

MODEL DESCRIPTION

The model is based on the incompressible Reynolds Averaged Navier-Stokes (RANS) equations:

Continuity Equation:

$$\partial_i u_i = 0 \tag{1}$$

Momentum Equation:

$$\partial_t u_i + u_j \partial_j u_i = -\partial_i p' + \nu \partial_{ii} u_i - \partial_j \overline{R_{ij}} + f_i \tag{2}$$

where u_i is the fluid velocity, p' the modified pressure, ν the kinematic viscosity, $\overline{R_{ij}} = \overline{u_i u_j}$ the Reynolds stresses and f_i is the body force.

Two-Equation Turbulence Models

Two-equation turbulence models are widely used in the CFD modelling of many industrial applications: they offer a good compromise between numerical effort and computational accuracy. They derive their name from the fact that they solve both the velocity and length scale using two transport equations.

The *k-ω* based two-equation model uses the gradient hypothesis to relate the Reynolds stresses to the mean velocity gradients and the turbulent viscosity.

$$-\overline{R_{ij}} = \nu_t \left(\partial_j \overline{u_i} + \partial_i \overline{u_j} \right) \tag{3}$$

The turbulent viscosity is defined as the product of a turbulent velocity and the turbulent length scale. In two-equation models, the turbulence velocity scale is computed from the turbulence kinetic energy (k) from the solution of a transport equation. The turbulent length scale is estimated from the turbulence kinetic energy and its dissipation rate (ε) or frequency (ω). The dissipation rate of the turbulence kinetic energy or turbulence frequency are provided from the solution of its own transport equation.

k-ω SST Turbulence Model

The transport equations for *k* and *ω* are given by equations (4) and (5), respectively (Menter et al., 2003)

$$\partial_t k + u_j \partial_j k = \partial_j \left((\nu + \sigma_k \nu_t) \partial_j k \right) + \min\left(P_k, 10\beta^* k\omega \right) - \beta^* k\omega, \tag{4}$$

$$\partial_t \omega + u_j \partial_j \omega = \partial_j \left((\nu + \sigma_\omega \nu_t) \partial_j \omega \right) + \alpha_\omega \frac{\omega}{k} \min\left(P_k, 10\beta^* k\omega \right) - \beta_\omega \omega^2 + 2(1 - F_1) \frac{\sigma_{\omega_{\phi 2}}}{\omega} \partial_j k \partial_j \omega. \tag{5}$$

The *k-ω* model does not account for the transport of the turbulent shear stress, which results in an over-prediction of eddy-viscosity, and ultimately leads to a failure in predicting the onset and the amount of flow separation from smooth surfaces. The proper transport behaviour can be obtained by using a limiter in the formulation of the eddy-viscosity and is given by

$$\nu_t = \frac{a_1 k}{\max\left(a_1 \omega, \mathbf{S}_{mag} F_2 \right)}, \tag{6}$$

where

$$\mathbf{S}_{mag} = \sqrt{2 S_{ij} S_{ij}}\ . \tag{7}$$

Each of the constants are a blend of an inner and outer constant, blended via

$$\phi = F_1 \phi_1 + (1 - F_1) \phi_2 \tag{8}$$

where ϕ_1 represents the inner constant and ϕ_2 the outer constant. The blending function F_1 is given by

$$F_1 = \tanh\left(\arg_1^4 \right), \tag{9}$$

with additional functions given by

$$\arg_1 = \min\left[\max\left(\frac{\sqrt{k}}{\beta^* \omega d}, \frac{500\nu}{d^2 \omega} \right), \frac{4\sigma_{\omega_{\phi 2}}}{CD_{k\omega} d^2} \right], \tag{10}$$

$$CD_{k\omega} = \max\left(\frac{2\sigma_{\omega_{\phi 2}}}{\omega} \partial_j k \partial_j \omega, 10^{-10} \right). \tag{11}$$

The second blending function, F_2 is given by

$$F_2 = \tanh\left(\arg_2^2 \right), \tag{12}$$

with

$$\arg_2 = \max\left(\frac{2\sqrt{k}}{\beta^* \omega d}, \frac{500\nu}{d^2 \omega} \right). \tag{13}$$

The model constants are $\beta^* = 0.09$ and $a_1 = 0.31$ with the remaining values shown in Table 1.

Table 1: SST model constants.

	α_ω	σ_k	σ_ω	β
ϕ_1	0.5556	0.85	0.5	0.075
ϕ_2	0.44	1.0	0.856	0.0828

Spalart and Shur Curvature Correction

One of the weaknesses of the eddy-viscosity models is that they are insensitive to streamline curvature, which plays a significant role in cyclone modelling. A modification of the turbulence production term is available to sensitize the standard eddy-viscosity models to these effects. A multiplier is introduced into the production term $(P_k \to P_k f_r)$ as given by Smirnov and Menter (2008)

$$f_r = C_{scale}\max\{\min(f_{rotation}, 1.25), 0.0\} \quad (14)$$

The empirical functions suggested by Spalart and Shur (1997) to account for these effects are given by

$$f_{rotation} = (1+c_{r1})\frac{2r^*}{1+r^*}\left[1-c_{r3}\tan^{-1}(c_{r2}\tilde{r})\right]-c_{r1}, \quad (15)$$

$$r^* = \frac{\mathbf{S}_{mag}}{\mathbf{\Omega}_{mag}}, \quad (16)$$

$$\tilde{r} = \frac{2\Omega_{ik}S_{jk}}{\mathbf{\Omega}_{mag}\mathbf{D}^3}\left(\frac{DS_{ij}}{Dt}+(\varepsilon_{imn}S_{jn}+\varepsilon_{jmn}S_{in})\Omega_m^{rot}\right), \quad (17)$$

$$S_{ij} = \frac{1}{2}(\partial_j u_i + \partial_i u_j), \quad (18)$$

$$\Omega_{ij} = \frac{1}{2}\left[(\partial_j u_i - \partial_i u_j) + 2\varepsilon_{mji}\Omega_m^{rot}\right], \quad (19)$$

$$\mathbf{S}^2 = 2S_{ij}S_{ij}, \quad (20)$$

$$\mathbf{\Omega}^2 = 2\Omega_{ij}\Omega_{ij}, \quad (21)$$

$$\mathbf{\Omega}_{mag} = \sqrt{2\Omega_{ij}\Omega_{ij}}, \quad (22)$$

$$\mathbf{D} = \max(\mathbf{S}^2, \beta^*\omega^2), \quad (23)$$

with constants $c_{r1}=1.0;\ c_{r2}=2.0;\ c_{r3}=1.0.$

Hellsten curvature correction

Hellsten (1998) derived an alternative simplified rotation/curvature correction to the SST model. The only modification requires the multiplication of the destruction term in the omega equation $(-\beta\omega^2)$ by the function F_4

$$F_4 = \frac{1}{1+C_{RC}R_i} \quad (24)$$

where the Richardson number is defined as

$$R_i = \frac{\mathbf{\Omega}_{mag}}{\mathbf{S}_{mag}}\left(\frac{\mathbf{\Omega}_{mag}}{\mathbf{S}_{mag}}-1\right) \quad (25)$$

with $\mathbf{S}_{mag}$ and $\mathbf{\Omega}_{mag}$ given by equations (7) and (22). The value of the constant C_{RC} has been set to 1.4 for this work following Mani et al. (2004). The formulation of R_i and the constant C_{RC} are chosen to ensure that F_4 always remains bounded. This allows the curvature correction to be treated implicitly in the omega equation, improving solver robustness.

Reynolds Stress Model

The Reynolds Stress Model (RSM) is applicable for the flows where the eddy-viscosity assumption is no longer valid and the results of eddy viscosity models might be inaccurate. They include the solution of transport equations for the individual components of the Reynolds stress tensor and the dissipation rate or turbulence frequency. The increased number of equations usually leads to reduced numerical robustness, increased computational time and restrictions for usability in complex flows. From the exact momentum equation a transport equation for the Reynolds stresses can be derived

$$\partial_t\overline{R_{ij}} + \overline{u_k}\partial_k R_{ij} = P_{ij} + \Pi_{ij} + D_{ij} - \varepsilon_{ij} \quad (26)$$

where P_{ij} is the production term, Π_{ij} is the pressure-strain correlation, D_{ij} is the diffusion term and ε_{ij} the dissipation term. The exact production term is given by

$$P_{ij} = -\overline{R_{ik}}\partial_k\overline{u_j} - \overline{R_{jk}}\partial_k\overline{u_i} \quad (27)$$

The dissipation is modelled as

$$\varepsilon_{ij} = \frac{2}{3}\varepsilon\delta_{ij} \quad (28)$$

with the turbulent dissipation rate coming from the turbulence kinetic energy and the turbulence frequency, $\varepsilon = \beta^* k\omega$. The "simple diffusion" model of Eisfeld (2004) is chosen to model the diffusion term

$$D_{ij} = \partial_k\left(\left(\nu + \frac{D\nu_t}{\beta^*}\right)\partial_k\overline{R_{ij}}\right) \quad (29)$$

with

$$D = 0.5\beta^* F_1 + 0.146(1-F_1) \quad (30)$$

The most important term in the RSM is the pressure-strain correlation (Π_{ij}) as it acts to drive turbulence towards an isotropic state by redistributing the Reynolds stresses. The model used in this work uses the Launder Reece Rodi (LRR) pressure-strain correlation from Launder et al. (1975) given by

$$\begin{aligned}\Pi_{ij} = &-C_1\varepsilon\overline{a_{ij}} + C_3 k\overline{S_{ij}}^* \\ &+C_5 k\left(\overline{a_{ik}}\,\overline{\Omega_{jk}} + \overline{a_{jk}}\,\overline{\Omega_{ik}}\right) \\ &+C_4 k\left(\overline{a_{ik}}\,\overline{S_{jk}} + \overline{a_{jk}}\,\overline{S_{ik}} - \frac{2}{3}\overline{a_{kl}}\,\overline{S_{kl}}\delta_{ij}\right)\end{aligned} \quad (31)$$

where $\overline{a_{ij}}$ is the anisotropy tensor defined as

$$\overline{a_{ij}} = \frac{\overline{R_{ij}}}{k} - \frac{2}{3}\delta_{ij} \quad (32)$$

and $\overline{S_{ij}}^*$ is defined as

$$\overline{S_{ij}}^* = \overline{S_{ij}} - \frac{1}{3}\overline{S_{kk}}\delta_{ij} \quad (33)$$

As with two-equation eddy viscosity models, an additional transport equation is required for closing the equation system for providing a measure of the isotropic dissipation rate ε. Most Reynolds stress models employ a transport equation for ε. The model used in this work follows Menter's (Menter, 1994) approach combining the ε equation at the outer edge of the boundary layer with the Wilcox (Wilcox, 1988) ω equation near the wall by blending coefficients. The so-called BSL-ω equation takes the form

$$\partial_t\omega + \overline{u_j}\partial_j\omega = \partial_j\left((\nu+\sigma_\omega\nu_t)\partial_j\omega\right) + \alpha_\omega\frac{\omega}{2k}\overline{R_{kk}} - \beta_\omega\omega^2 \quad (34)$$

The constants are defined in Table 2 with $C_2^{LRR}=0.52$.

Table 2: LRR model constants.

C_1	C_3	C_4	C_5
1.8	0.8	$\frac{9C_2^{LRR}+6}{11}$	$\frac{-7C_2^{LRR}+10}{11}$

LES

Large Eddy Simulation (LES) computes the large-scale motions of the flow directly. The small-scale, dissipative motions of turbulence tend to more amenable to modelling because of their more uniform character, whereas the large-scale motions contain the majority of the energy and anisotropy. As a result, LES is expected to be more accurate, particularly in complex flows where the assumptions inherent to RANS models rarely exist. The drawback is that LES simulations are always three-dimensional and unsteady.

Smagorinsky

The Smagorinsky model (Smagorinsky, 1963) determines the unknown stresses $\tau_{ij} = -2\nu_{SGS}S_{ij}$ by an algebraic model for the subgrid scale (SGS) viscosity (ν_{SGS}). The SGS viscosity can be calculated as

$$\nu_{SGS} = C_s^2 \Delta^2 \mathbf{S}_{mag} \tag{35}$$

where Δ represents the top-hat filter with a characteristic filter width estimated as the cubic root of the cell volume. In this work the value used for C_s was 0.1.

Coherent structure

The coherent structure LES model was introduced by Kobayashi (2005). The main idea of the model consists of the local determination of the model constant C_s used in the SGS model. The model constant is defined through a coherent structure function F_{CS} through the following expression

$$C_s^2 = C_{CSM} \left| F_{CS} \right|^{3/2} \left(1 - F_{CS}\right) \tag{36}$$

The coherent structure function is given by the second invariant Q normalised by the magnitude of shear

$$F_{CS} = \frac{Q}{E} \tag{37}$$

$$Q = -\frac{1}{2}\partial_i \overline{u}_j \partial_j \overline{u}_i \tag{38}$$

$$E = \frac{1}{2}\left(\partial_i \overline{u}_j\right)^2 \tag{39}$$

with the model constant $C_{CSM} = 1/22$.

The coherent structure model is particularly well suited for rotating flows and it is comparable with the dynamic SGS model (Germano et al., 1991). However, unlike the dynamic model, the coherent structure uses only the local information and it is computationally cheaper. In addition, the model is suitable for the simulations on complex geometries when there are no homogeneous directions in which it is possible to perform averaging.

FLOW CONFIGURATION

The cyclone (Figure 1) features an outer diameter 0.39 m and a half-angle of 20° in the conical region and a pipe outlet at the bottom end for collecting particles. This outflow is closed for all simulations to match the experimental operating conditions. Hence all the flow exited through the vortex finder at the top of the cyclone. Flow enters the cyclone through a tangential inlet attached to the cylindrical section.

The grid consisted of 606,264 hexahedral elements arranged to achieve good cell quality. At the inlet a uniform velocity of 21.5 m/s with turbulence quantities calculated from mixing length theory are applied. A Neumann condition was applied to all flow quantities at the vortex finder outlet. Zero velocity is assumed on all walls were an adaptive wall function is used.

NUMERICAL METHOD

The conservation equations of mass, momentum and turbulence given above were solved using a finite volume method in order to determine the single-phase liquid velocity for comparison against the experimental data. A transient solver implemented in v5.04 of the Caelus library (Applied CCM, 2015) was used. Pressure-velocity coupling was achieved via the SLIM algorithm (Sideroff et al., 2015). For the discretization of time-dependent terms, the 2nd order backward scheme was used. Pressure and velocity gradients were calculated using the Green-Gauss method. A 2nd order linear upwind discretization with multidimensional interpolation linear scheme utilising Barth-Jespersen limiter (Berger at al., 2005) was used for the advection terms. A steady-state solution using the *k-ω* SST turbulence model was used to initialise each of the transient simulations. A time step that gave a maximum Courant number of five (giving a mean ~ 0.5) was used for simulations using all turbulence models except RSM. For stability, the RSM simulation required the maximum Courant number to be limited to 0.5. The procedure used for each simulation was to run for an initial time of ~50 residence times, followed by a further 1000 residence times where the simulations data were time averaged. The initial time period was determined to be sufficient for the flow to develop. Time averaging over the remaining time appeared to be sufficient a length for statistical sampling of mean quantities.

All simulations were conducted on a HPC cluster utilising 60 Intel Xeon E5-2620v3 cores per simulation. Infiniband was used for communication between the cluster compute nodes. Table 3 shows a comparison of the CPU time (hour) for each model to simulate 1 second of flow time.

Table 3: Comparison of CPU time to simulate 1s of flow for each turbulence model.

Model	CPU time (hour) per 1s flow time
SST	1.01
SST-CC	1.14
SST-HELL	1.05
SMAG	1.18
CS	1.48
RSM-LRR	10.90

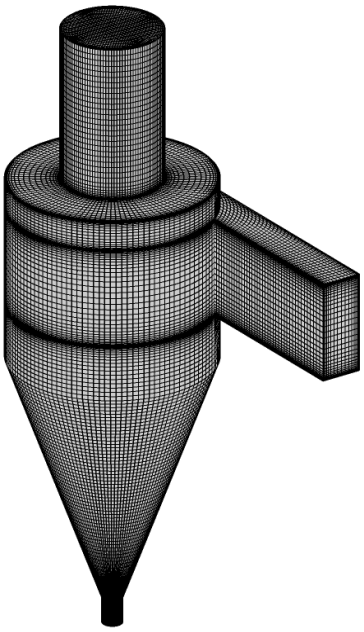

Figure 1: Cyclone geometry and surface mesh.

RESULTS

Data from Laser Doppler Velocimetry (LDV) measurements of gas velocities along horizontal traverses at various heights are presented in Witt et al. (1999). These data along with simulation results for the tangential and vertical velocities at six vertical heights from this work are presented in Figures 2 and 3. In these figures the results have been non-dimensionalised by the cyclone radius and inlet velocity. The measurement positions were located at a circumferential location 90° in the direction of flow from the point where the inlet duct is attached. The vertical locations A, B and C are positioned above the join between the cylindrical and conical sections at non-dimensional distances of 1, 0.75 and 0.125 respectively. Locations D, E and F are positioned below the join at non-dimensional distances of 0.25, 0.75 and 1.25 respectively. The vortex finder wall is located at a non-dimensional radius of 0.48. Results for each turbulence model are shown on these figures with the following labels, SST – *k-ω* SST model, SST-CC – Spalart and Shur curvature correction applied to the *k-ω* SST model, SST-HELL – Hellsten curvature correction applied to the *k-ω* SST, SMAG – LES simulation using the Smagorinsky SGS model, CS – LES simulation using the coherent structure SGS model and RSM-LRR – RSM simulation using the LRR pressure-strain correlation.

The tangential velocities predicted by SST show significant deviation from the experimental measurements at all vertical locations, especially in the region near the outer wall of the cyclone. This result is not unexpected as Stephens and Mohanarangam (2010) showed that without modification the model was inaccurate for highly swirling flows. SST-HELL results also show significant deviation from the experimental profiles at all locations, following a similar profile to the SST results. SST-CC results show quite different profiles compared with the SST and SST-HELL results, with better agreement with the experimental profiles, although with a lower velocity magnitude. Tangential velocity results from the two LES simulations (SMAG and CS) show excellent agreement with the experimental profiles at all six measurement locations. Only minor differences can be observed between the SMAG and CS results with these occurring near the centreline of the cyclone. The RSM simulation results mirror those of SST-CC, having the correct profile shape but lower magnitude than the experimental measurements.

Vertical velocity results show similar trends between turbulence models as observed for the tangential velocities, i.e. SST and SST-HELL do not recover the experimental profiles. Again the SST-CC results show significant difference to the SST and SST-HELL, but match the experimental data reasonably well. The region with the largest discrepancy is the centreline where the experiments show a much stronger downward velocity than the model predicts. Like the tangential case, the SMAG and CS profiles are very similar, but only at the higher measurement locations (A, B and C). The profiles begin to deviate as you move lower down in the cyclone. A difference between the model predictions can be seen near the centreline for all measurement locations, with the CS model having better agreement with the experimental data at all locations. The RSM results again match the experimental profiles and magnitudes reasonably well.

Overall the SST and SST-HELL predictions are poor. The SST-CC provides a significant improvement to the standard SST, however, there are still deficiencies in the model's predictions, e.g. lower tangential magnitude and failure to capture the downward velocity at the cyclone centreline. Whilst the RSM model offers no better tangential velocity predictions compared with SST-CC, it does better at predicting the downward flow at the cyclone centreline. This marginal improvement over the SST-CC comes at a much higher computational cost (see Table 3) due to the additional five equations and the reduced time step size required for stability. The SMAG tangential results are in excellent agreement with the measurements, however, in the lower region (locations D, E, and F) it fails to capture downward velocity. The CS model gives the overall best agreement with the measurements for both the tangential and vertical velocities at all six measurement locations.

To allow comparison of different cyclone designs, the pressure drop from cyclone inlet to outlet can be non-dimensionalised producing a pressure loss coefficient. The pressure loss coefficient is defined as

$$\xi = \frac{p'_{in} - p'_{out}}{\frac{1}{2}u_{in}^2} \tag{40}$$

Comparison of the predicted pressure loss coefficient with the measurement value can be seen in Table 4. It can be seen that CS gives the closest prediction to the measurement, followed by SMAG, RSM-LRR, SST-CC, SST-HELL and SST.

Table 4: Pressure loss coefficient from experiment and simulations for each turbulence model.

	EXP	SST	SST-CC	SST-HELL	SMAG	CS	RSM-LRR
ξ	6.80	10.2	6.02	8.77	6.19	6.56	6.09

CONCLUSION

Analysis of different turbulence models was carried out for a turbulent flow inside cyclone. Six different turbulence models were tested of which three belong to the two-equation model class, two to the LES class and one to the Reynolds Stress class. Simulations were performed with a transient solver using version 5.04 of the Caelus library. Experimental results of Witt et al. (1999) were used to compare our numerical findings. For the different turbulence models tested, the coherent structure (CS) LES gave the best overall prediction. The k-ω SST model without any curvature correction produced the poorest predictions of the flow field The LRR Reynolds Stress model offered a marginal improvement over the SST-CC with the penalty of much higher computational cost due to the additional five equations and reduced time step size for stability.

REFERENCES

APPLIED CCM (2015). Caelus: Computational Mechanics Library (Version 5.04) [Software], available at http://www.caelus-cml.com.

BOYSAN, F., AYER, W.H., and SWITHENBANK, J. A. (1984). "Fundamentals mathematical-modeling approach to cyclone design", *Trans. Inst. Chem. Eng.*, **60**, 222-230.

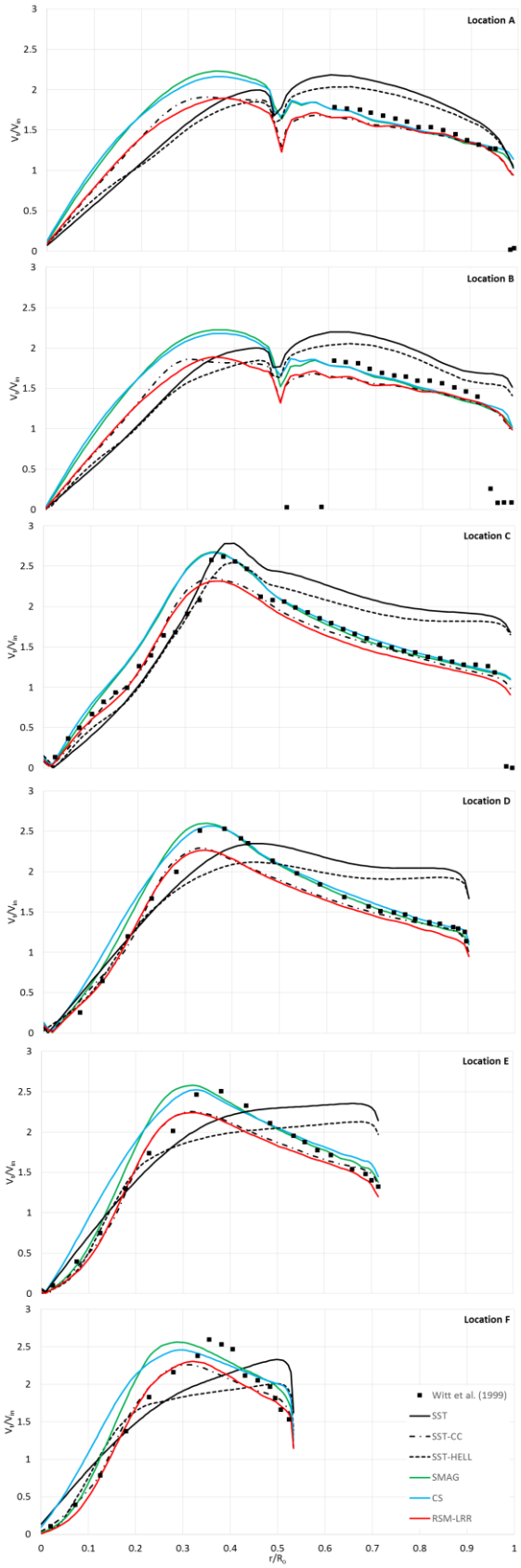

Figure 2: Time-averaged tangential velocity profiles at six measurement locations.

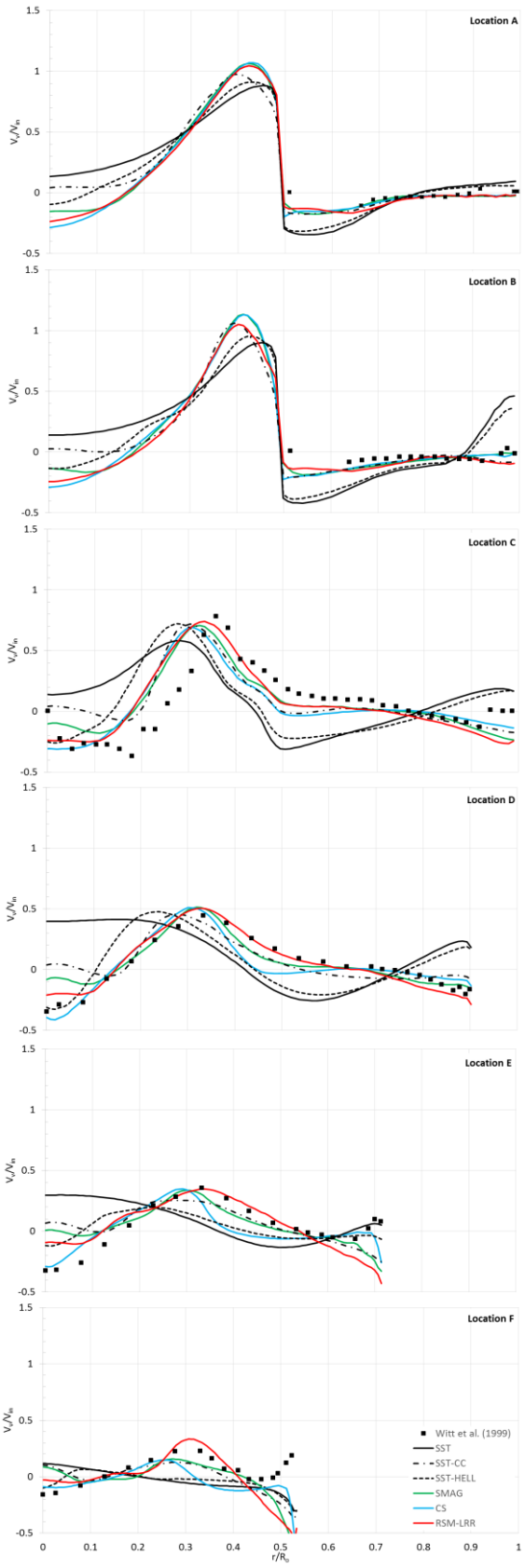

Figure 3: Time-averaged vertical velocity profiles at six measurement locations.

BERGER, M., AFTOSMIS, M.J., and MURMAN, S. M. (2005). "Analysis of slope limiter on irregular grids", *43rd AIAA Aerospace Sciences Meeting*, Jan. 10-13, Reno, NV

EISFELD, B. (2004). "Implementation of Reynolds Stress models into the DLR-FLOWer Code", Institutsbericht, DLR-IB 124-2004/31, Report of the Institute of Aerodynamics and Flow Technology, Braunschweig, ISSN 1614-7790.

GERMANO, M., PIOMELLI, U., MOIN, P., and CABOT, W. H. (1991). "A dynamic subgrid-scale eddy viscosity model", *Phys. Fluids A*, **3**, 1760-1765.

HELLSTEN, A. (1998). "Some improvements in Menter's k-omega SST Turbulence Model", *AIAA paper 98-2554*.

KOBAYASHI, H. (2005). "The subgrid-scale models based on coherent structures for rotating homogeneous turbulence and turbulent channel flow", *Phys. Fluids*, **17**, 2005.

LAUNDER, B.E, REECE, G.J. and RODI, W., (1975). "Progress in the development of a Reynolds-stress turbulence closure", *J. Fluid Mech.*, **68**, 537–566.

MANI, M., LADD, J.A. and BOWER, W.W. (2004). "Rotation and curvature correction assessment of one- and two-equation turbulence models", *J. Aircraft*, **41(2)**, 268-73.

MENTER, F.R. (1994). "Two-equation eddy-viscosity turbulence models for engineering applications", *AIAA Journal*, **32(8)**, 1589-1605.

MENTER, F.R., KUNTZ, M., and LANGTRY, R. (2003). "Ten years of industrial experience with the SST turbulence models", *Turbulence, Heat and Mass Transfer 4*, Begell House Inc., 625–632.

SIDEROFF, C., STEPHENS, D.W., and JEMCOV, A. (2015). "A projection method based fast transient solver for incompressible turbulent flows", *23rd Annual Conference of the CFD Society of Canada*, June. 7-10, Waterloo, Canada.

SMAGORINSKY, J. (1963) "General circulation experiments with the primitive equations. I. The basic experiment", *Mon. Weather Rev.*, **91**, 99-152.

SMIRNOV, P.E. and MENTER, F.R. (2008). "Sensitization of the SST turbulence model to rotation and curvature by applying the Spalart-Shur correction term", *ASME Paper GT 2008-50480*. Berlin, Germany.

SPALART, P.R. and SHUR, M. (1997). "On the sensitization of turbulence models to rotation and curvature", *Aerospace Science and Technology*, **1**(5), 297-302.

STEPHENS, D.W. and MOHANARANGAM, K. (2010). "Turbulence model analysis of flow inside a hydrocyclone", *Progress in CFD*, **10(5/6)**, 366-373.

WILCOX, D.C. (1988). "Reassessment of the scale-determining equation for advanced turbulence models", *AIAA Journal*, **26(11)**, 1299-1310.

WITT, P.J., MITTONI, L.J., WU, J., SHEPHERD, I.C. (1999). "Validation of a CFD model for predicting gas flow in a cyclone", In: Chemeca 99: Chemical Engineering: Solutions in a Changing Environment. [Barton, A.C.T]: Institution of Engineers, Australia, 246-251.

